Electronic Supplementary Information (ESI)

Active-passive Strategy for Enhanced Synergistic Photothermal-Ferroptosis Therapy in NIR-I/II Biowindows

Fengxia Wu,[a, b] Haoran Chen,[b] Ruiqi Liu,[a] Yongkuan Suo,[a] Qiqing Li,[b] Youlin Zhang,[b] Hongguang Liu,[a] Zhen Cheng,*[c] and Yulei Chang*[b]

a. Institute of Molecular Medicine, College of Life and Health Sciences, Northeastern University, Shenyang, Liaoning 110169, China.

b. State Key Laboratory of Luminescence and Applications. Changchun Institute of Optics, Fine Mechanics and Physics, Chinese Academy of Sciences, Changchun, 130033, Jilin, China. Email: yuleichang@ciomp.ac.cn

c. Molecular Imaging Program at Stanford, Stanford University, Palo Alto, CA, USA. Email: zcheng@stanford.edu

Experimental

Materials

Bismuth(III) acetate ($(CH_3CO_2)_3$, ≥99.99%) was purchased from Sigma-Aldrich Chemicals, Sodium selenite (Na_2SeO_3, 98%) was obtained from Xiya Chemical Technology Co., Ltd. (Shandong, China). Polyvinylpyrrolidone (PVP, Mw≈40,000), the ethylene glycol (EG, >99.0%), triethylene glycol (TEG, >99.0%), hydroxylamine solution (50 wt. % in H_2O), acetic acid (AA, ≥99.5) and Iron (III) acetylacetonate ($Fe(acac)_3$, >98.0%) were purchased from Aladdin (Shanghai, China). Deferoxamine mesylate (DFO, >99.0%) was purchased from MedChemexpress CO., Ltd. (Shanghai, China). Reduced glutathione (GSH) assay kit and cell apoptotic assay kit were purchased from Solarbio (Beijing, China). Liperfluo probe was purchased from Dojindo (Beijing, China). All the chemicals were used as received without further purification.

Synthesis of Bi_2Se_3 nanosheets

The Bi_2Se_3 nanosheets were prepared by a solvothermal method.[31] Typically, 0.3 mmol $Bi(AC)_3$ and 0.4 g PVP were dissolved in 10 mL EG in a 50 mL three-neck flask. Then, 0.45 mmol Na_2SeO_3 and 1 mL AA were placed into the flask. The mixture was kept stirring until a clear solution was formed. Afterward, when the solution was heated to 170 °C, 2 mL of hydroxylamine solution and ethylene glycol (1:1) were rapidly injected into the above solution, which was immediately turned black, the reaction was kept at 170 °C for 15 min. After cooling to room temperature, the product was precipitated by the addition of 20 mL acetone, collected via centrifugation at 8,000 rpm for 10 min, subsequently washed twice with acetone. The final product was dispersed in water for further use.

Synthesis of Bi_2Se_3-Fe_3O_4 NPs

To obtain the Bi_2Se_3-Fe_3O_4 composites, a thermal decomposition method was employed by decomposing the $Fe(acac)_3$ in the presence of Bi_2Se_3 nanosheets. Briefly, 8 mg of $Fe(acac)_3$ and 5 mg of Bi_2Se_3 nanosheets were added to 30 mL of TEG by ultrasonication and magnetic stirring. Afterwards, the mixture was placed in a 50 mL Teflon-lined stainless steel autoclave, sealed, and maintained at 220 °C for 10 h. After that, the products were collected by centrifugation and washed three times with absolute ethanol.

Synthesis of Bi_2Se_3-Fe_3O_4/Au (BFA) NPs

The Bi_2Se_3-Fe_3O_4/Au (BFA) NPs were prepared by a sodium citrate reduction method of $HAuCl_4$. Briefly, sodium citrate (200 μL, 7.05 mg mL^{-1}) was added to the 6 mL Bi_2Se_3-Fe_3O_4 solution, then, a solution of $HAuCl_4$ (1%) was added while stirring. After 15 min, the products were collected by centrifugation and dispersed in water for further use. To improve the biocompatibility and stability, the PEG moieties were coupled to the surface of BFA NPs. Briefly, PEG-NH_2 (M.W 2000) at a mass ratio of 1:5 was added into the BFA NPs solution (2 mg mL^{-1}) under magnetic stirring at room temperature. After stirring for 24 h, the products were collected by centrifugation and re-dispersed in distilled water for further use.

Photothermal performance of BFA NPs

The BFA NPs solutions with different concentrations (0, 10, 20, 40 and 80 μg mL^{-1}) in a transparent cuvette, irradiated by 808 or 1064 nm laser (1 W cm^{-2}, 10 min) and recorded the temperature every 30 s. Similarly, to assess the photostability of BFA NPs, the sample (80 μg mL^{-1}) was irradiated for 10 min with an 808 or 1064 nm laser, then cooled to room temperature with the laser off. The laser on/off for 5 cycles and recorded the temperature every 30 s.

Photothermal conversion efficiency

The photothermal conversion efficiency (η) of BFA NPs was calculated according to the previous reports.[1,2]

$$\sum_i m_i C_{p.i.} \frac{dT}{dt} = Q_{Bi2Se3-Fe3O4/Au} + Q_s - Q_{loss} \quad (1)$$

$$\eta = \frac{hA(\Delta T_{max} - \Delta T_{H2O})}{I(1 - 10^{-A808/1064})} \quad (2)$$

$$\theta = \frac{\Delta T}{\Delta T_{max}} \quad (3)$$

$$t = -\frac{\sum_i m_i C_{p,i}}{hA} ln\theta \quad (4)$$

where m_i and $C_{p,i}$ are the mass and heat capacity of the solvent (water), Q_s is the heat which is absorbed by the water, Q_{loss} is the thermal energy transferring to the environment, ΔT_{max}, ΔH_2O are the maximal

temperature change of BFA NPs solution and DI Water. *I* is the laser power, $A_{808/1064}$ means the absorbance of BFA NPs at the wavelength of 808 or 1064 nm. To calculate the photothermal conversion efficiencies (η), according to Equation (2, 4), plotting curves of time (s) and $-ln\theta$ in the cooling stage, there is a negative correlation between *hA* and slope.

The peroxidase-like activity of BFA NPs

In this work, we choose the TMB (0.4 mM) as the peroxidase substrate to explore the catalytic activity of BFA NPs, the absorbance of oxTMB was monitored at 652 nm using an absorption spectrum instrument. The citric acid-sodium citrate buffer (0.1 M, pH = 4) is the reaction solution. For the H_2O_2 specific, there are three groups (TMB + H_2O_2; TMB + BFA NPs; TMB + BFA NPs + H_2O_2), the reaction was carried out at 37 °C for 30 min.

Michaelis-Menten kinetic analysis of Bi_2Se_3-Fe_3O_4 and BFA NPs

For the study steady-state kinetic, the same amount of Bi_2Se_3-Fe_3O_4 /BFA NPs (20 μg mL^{-1}) reacted with different concentrations of H_2O_2 (10, 20, 30, 40, 50 mM) in 2 mL citric acid -sodium citrate buffer (pH = 4), 0.4 mM TMB, the reaction was carried out in 37 °C for 15 min.

Cell culture

4T1 cells (Murine breast carcinoma cells), A549 cells (Human lung adenocarcinoma cells), and RAW 264.7 cells (Leukemia cells in mouse macrophage) were obtained from the Institute of Basic Medicine, Chinese Academy of Medical Science. 4T1 cells and A549 cells were cultured in RPMI-1640 culture medium and RAW 264.7 cells were grown in Dulbecco's modified Eagle's medium (DMEM), containing 10% fetal bovine serum (FBS) and 1% penicillin/streptomycin at 37 °C with 5% CO_2.

Anti-tumor effect *in vitro*

RAW 264.7 and 4T1 cells (1.0×10^4/well) were seeded into the 96-well plates and cultured overnight, then incubated with various concentrations of Bi_2Se_3-Fe_3O_4 and BFA NPs (0, 12.5, 25, 50, 100, 200 μg mL^{-1}), respectively. After incubation for 24 h, the culture medium was replaced by fresh DMEM or RPMI-1640 containing 10% CCK-8 and incubated for another 1-2 h. Finally, evaluate the cell viability by measuring the absorbance of wells at 450 nm. For the PTT-ferroptosis synergistic therapy *in vitro*, 4T1 cells (1.0×10^4/well) were seeded into the 96-well plates and cultured overnight. Then, the 4T1 cells were treated with BFA NPs (100, 200 μg mL^{-1}) for 12 h before irradiation by 808 nm (0.5 W cm^{-2}, 5 min) or 1064 nm (1.0 W cm^{-2}, 5 min) laser. After further incubation for 12 h, the cytotoxicity was evaluated by the CCK-8 assay.

Reactive oxygen species (ROS) generation *in vitro*

The intracellular ROS was detected by an oxidation-sensitive fluorescent probe (DCFH-DA). Briefly, 4T1 cells were seeded into the 20-mm dishes at a density of 1.0×10^5 per plate and cultured overnight. The 4T1 cells divided into three groups with different treatments: (a) PBS; (b) BFA NPs (100 μg mL^{-1}); (c) BFA NPs (100 μg mL^{-1}) + DFO (100 μM). After 6 h, the culture medium was replaced by 1 mL DCFH-DA (10 μM in FBS-free RPMI-1640) and incubated for 30 min, afterward, the cells were washed three times with RPMI-1640 (FBS free). Subsequently, the production of reactive oxygen species (ROS) was evaluated by measuring the fluorescence of DCF (ex/em = 488/525 nm) with a CLSM (Nikon).

Intracellular glutathione (GSH) level and lipid hydroperoxide (LPO) assay

The intracellular GSH level was estimated by a reduced glutathione assay kit. Briefly, 4T1 cells at a density of 1.0×10^5 per plate were seeded into the 20-mm dishes and cultured overnight. The 4T1 cells divided into three groups with different treatments: (a) PBS; (b) BFA NPs (100 μg mL^{-1}); (c) BFA NPs (100 μg mL^{-1}) + DFO (100 μM). After incubation for 6 h, the cells were washed with PBS three times, collected, and measured the GSH level according to the manufacturer's instructions.

For Intracellular LPO detection, 4T1 cells were incubated with a Liperfluo probe (5 μM) for 30 min at 37 °C. Finally, the fluorescence was observed with CLSM after staining the cell nuclei with DAPI.

Western blotting

The protein samples were collected from 4T1 cells for SDS-PAGE (12%), then transferred onto a 0.45 μm nitrocellulose membrane. After being blocked with blocking buffer, the membranes were incubated with GPX4 rabbit polyclonal antibody (1:1000) and β-actin mouse monoclonal antibody (1:1000) overnight at 4 °C. The membrane was incubated with secondary antibodies (AP-labeled Goat Anti-Rabbit IgG, 1:1000) for 1 h at room temperature. Finally, the BCIP/NBT Alkaline Phosphatase Color Development Kit (Beyotime Biotechnology) performed the detection, and then the scanner (Canon, Japan) scanned the blots.

Real-time quantitative polymerase chain reaction (RT-qPCR)

Total RNA was extracted from 4T1 cells treated with BFA NPs and then cDNA synthesis was performed using a reverse transcription Kit (TAKARA BIO INC.). Quantitative real-time PCR was performed with the

Real-time PCR System using PCR Kit (TAKARA BIO INC.). The primer pairs were shown as follows: GPX4 forward (5'-ACC GAA GTA AAC TAC ACT CAG-3') and reverse (5'-GGC GAA CTC TTT GAT CTC TT-3'); β-actin forward (5'-CACCATTGGCAATGAGCGGTTC-3') and reverse (5'-AGGTCTTTGCGGATGTCCACGT-3').

Determination of mitochondrial membrane potential

The mitochondrial membrane potential was evaluated by JC-1 assay. Briefly, 4T1 cells were seeded in 20 mm dishes and cultured overnight. Then, the cells were divided into 5 groups including: (a) PBS; (b) laser only; (c) BFA NPs; (d) BFA NPs + DFO; (e) BFA NPs + laser. After 6 h incubation, the JC-1 assay was performed according to the manufacturer's instruction and observed by CLSM.

Cell apoptosis assay

The cell apoptosis was assessed by annexin V-FITC/PI double staining according to the apoptotic assay kit. 4T1 cells were seeded in six-well plates at the density of 5×10^5 cells per well and cultured overnight. After the different treatments, the cells were suspended in the PBS buffer and centrifuged at 1000 rpm for 5 min to remove the supernatants. Then, the cells were resuspended in 100 μL of binding buffer and stained with 5 μL of annexin V-FITC and 5 μL of PI kept away from light for 15 min at room temperature. Finally, the fluorescence intensities of the samples were monitored by flow cytometry.

Bio-transmission electron microscopy (Bio-TEM)

4T1 cells were seeded in culture plates and cultured overnight. Then the cells were collected after treated with PBS or BFA NPs for 10 h. Subsequently, the cells were fixed with 2.5% glutaric dialdehyde solution for bio-TEM imaging.

Mouse tumor model

Female Balb/c mice (6-8 weeks) were purchased from Vital River Company in Beijing. All animal experiments were observed in the Animal care and Use Committee of Northeastern University. The 4T1 cell suspension (2.0×10^6/tumor, in saline medium), was subcutaneously injected into the right flank of each mouse. When the tumor volumes reached about 60 mm^3, the *in vivo* experiments were then conducted.

PA/MR imaging *in vitro* and *in vivo*

In vitro and *in vivo* PA/MR imaging was acquired by the photoacoustic imaging system (Endra Nexus 128) and 1.2 T MRI scanner (HT-MRSI15-50KY). For *in vitro* PAI, BFA NPs were dispersed in an aqueous with different concentrations. For *in vivo* PA imaging, 4T1 tumor-bearing mice intravenously injected with BFA NPs (200 μL, 2 mg mL^{-1}) were measured at different times (0, 2, 4, 8, 12, and 24 h) after anesthetized with 5% chloral hydrate. For *in vitro* MRI, BFA NPs at various concentrations of iron were dispersed in an aqueous solution. The values of $1/T_2$ were linearly fitted to corresponding iron concentrations, to calculate the r_2 value of BFA NPs. For *in vivo* MRI, 4T1 tumor-bearing mice intravenously injected with BFA NPs (200 μL, 2 mg mL^{-1}) and T_2-weighted images were obtained at different times.

X-ray imaging *in vivo*

For X-ray imaging *in vivo*, 4T1 tumor-bearing mice with intratumoral injection of 50 μL BFA NPs (2 mg mL^{-1}) were scanned by the X-ray imaging system (MultiFocus, Faxitron, USA).

Synergistic anti-tumor effect *in vivo*

4T1 tumor-bearing mice (n = 3) randomly divided into 4 groups, including: (a) PBS; (b) PBS + laser (808 nm, 0.5 W cm^{-2}, 10 min); (c) BFA NPs (20 mg/kg); (d) BFA NPs (20 mg/kg) + laser (808 nm, 0.5 W cm^{-2}, 10 min). The tumor size and body weights were measured every two days, the tumor volume was calculated following the equation: Volume = (Tumor Length) × $(\text{Tumor Width})^2/2$. For the biocompatibility evaluation, after 21 days of treatments, collect the major organs (heart, liver, spleen, lung, and kidney) for further H&E assay.

Tumor tissues analysis

After different treatments, tumor tissues were collected and histopathologically analyzed by H&E, TUNEL staining and LPO detection, and then pictures were collected by fluorescence microscope.

Statistical analysis

All experimental data were assessed as mean ± standard deviation (SD). The differences between the two groups were determined using a two-tailed Student's t-test using origin 7 and statistical significance was $^*P < 0.05$.

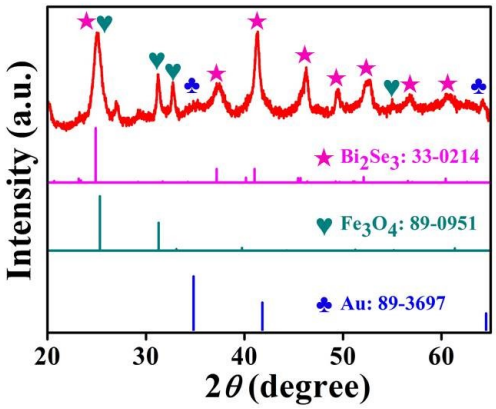

Fig. S1 X-ray diffraction (XRD) of Bi_2Se_3-Fe_3O_4/Au (BFA) NPs.

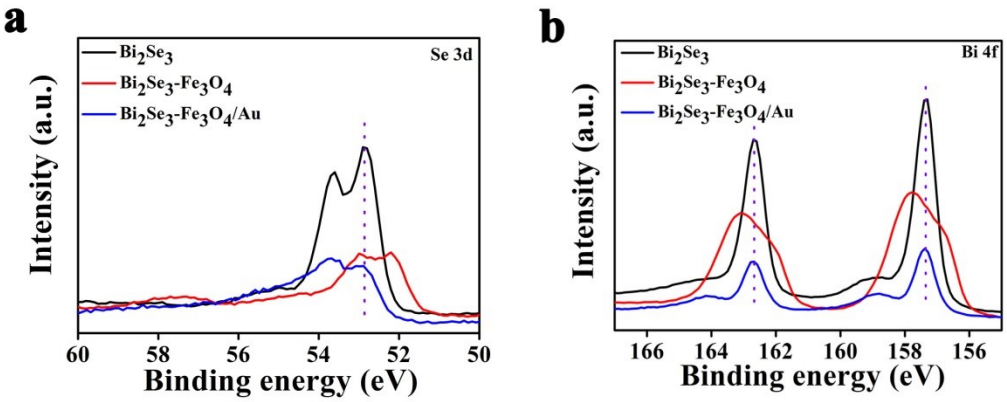

Fig. S2 High-resolution XPS spectra of (a) Se 3d and (b) Bi 4f.

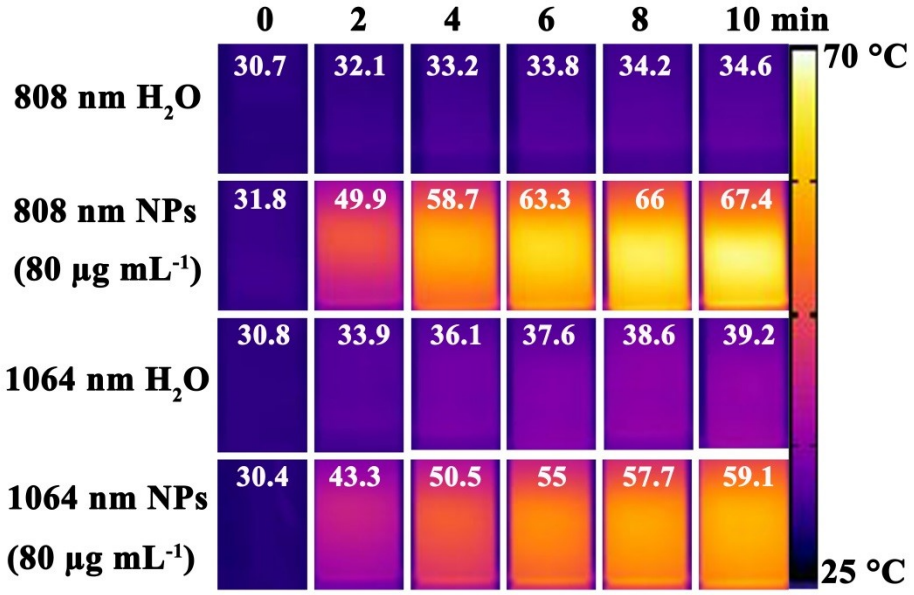

Fig. S3 Representative thermal images of DI Water and BFA NPs (80 μg mL $^{-1}$) at different times under 808 or 1064 nm laser irradiation (1 W cm^{-2}).

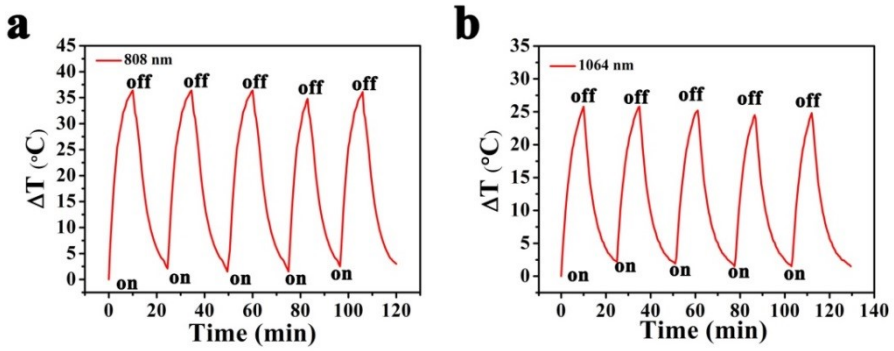

Fig. S4 Photostability curves of Bi_2Se_3-Fe_3O_4/Au solution for five on/off cycle under the irradiation of (a) 808 or (b) 1064 nm laser.

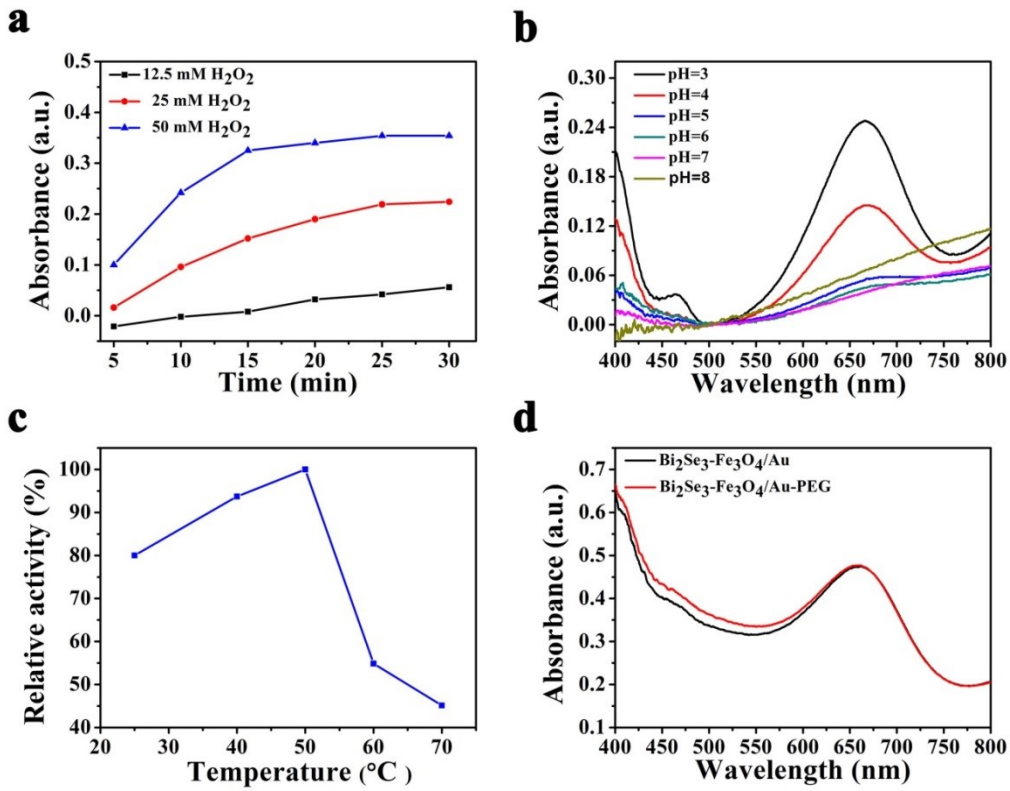

Fig. S5 (a) The time-dependent absorbance changes at 652 nm with the varied concentration of H_2O_2. The effects of (b) pH and (c) temperature on the catalytic activity of BFA NPs. (d) UV-Vis spectra of the oxTMB under the catalyzed of BFA NPs and BFA-PEG NPs.

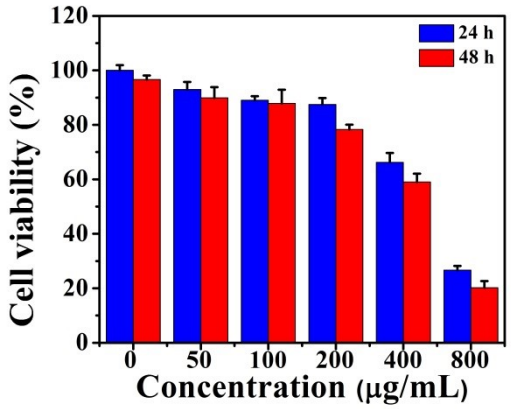

Fig. S6 Relative cell viability of 4T1 cells treated with BFA NPs with different concentrations (0, 50, 100, 200, 400, 800 μg mL^{-1}) for 24 h and 48 h.

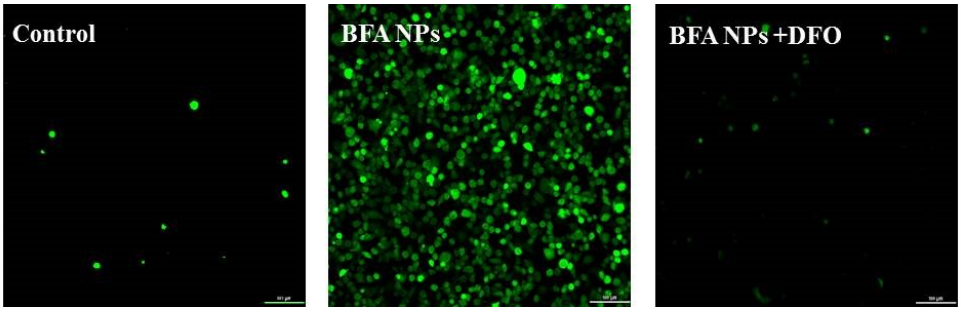

Fig. S7 Confocal images of DCFH-DA (2, 7-dichlorofluorescein diacetate) stained A549 cells under different treatments. Scale bar: 100 μm.

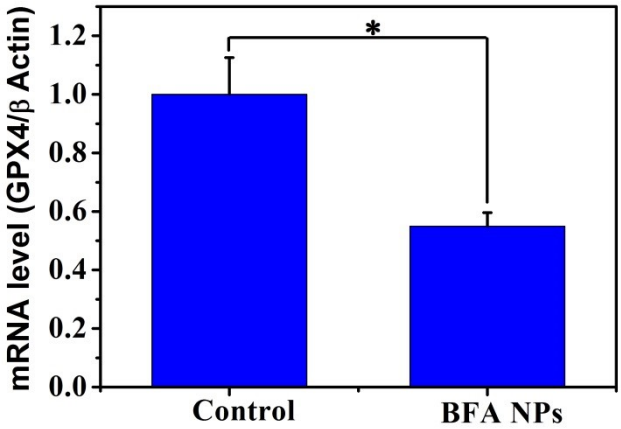

Fig. S8 Intracellular mRNA level of GPX4 in 4T1 cells treated with PBS and BFA NPs. The data are shown as the mean s. d. (n = 3). ***p < 0.001, **p < 0.01, *p <0.05.

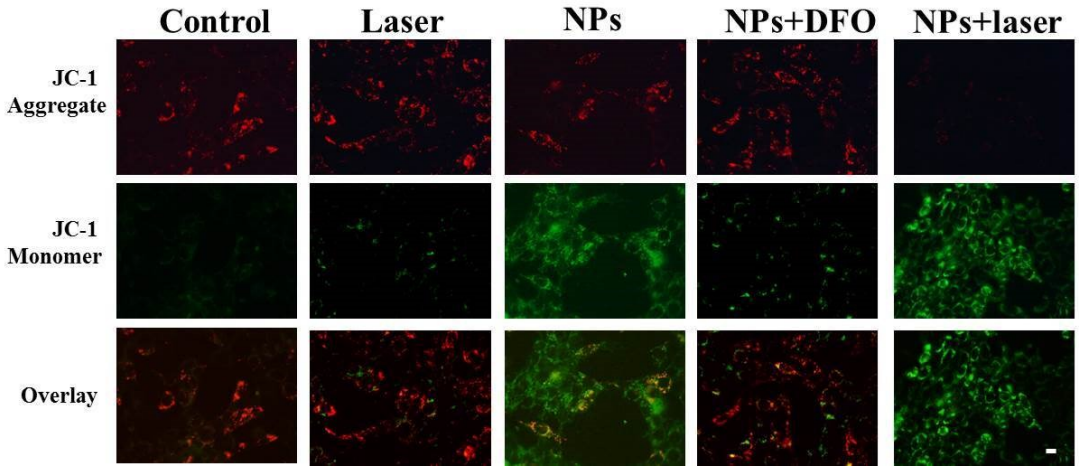

Fig. S9 CLSM images of Δψm in 4T1 cells after different treatments. Scale bar: 10 μm.

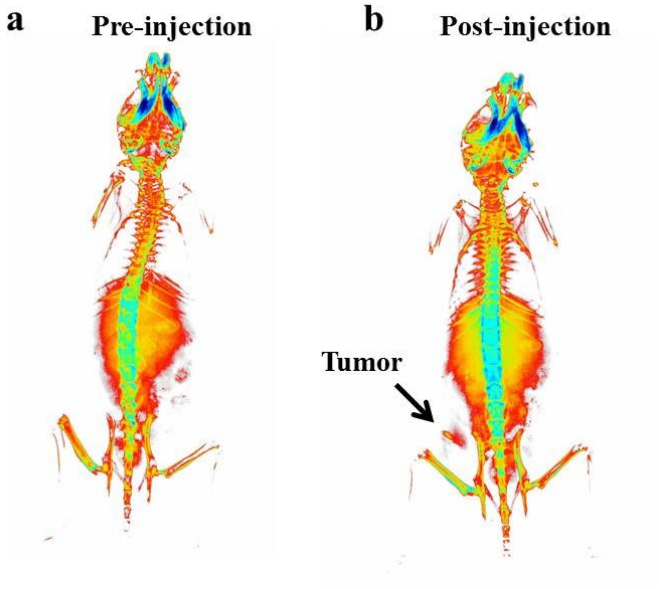

Fig. S10 The X-ray images of 4T1 tumor-bearing mice (a) before and (b) after injection of BFA NPs (i.t.).

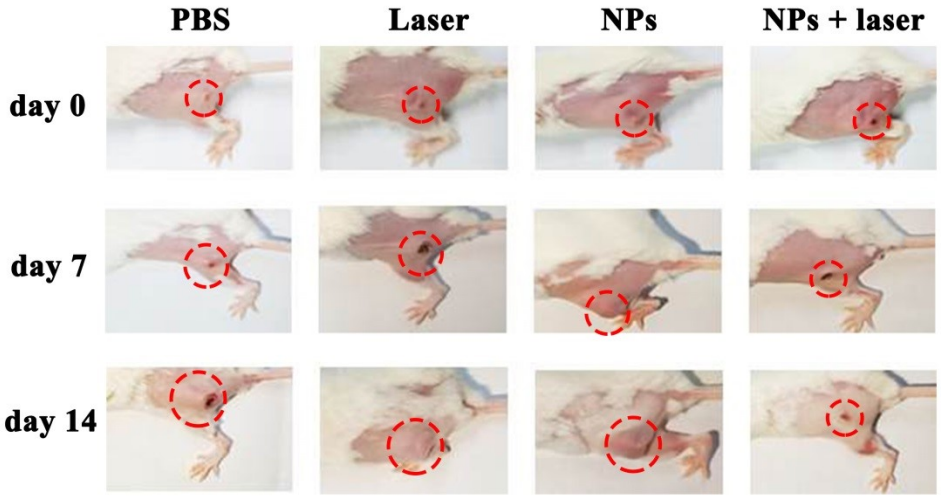

Fig. S11 Representative photos of tumor-bearing mice in different groups during the therapeutic period.

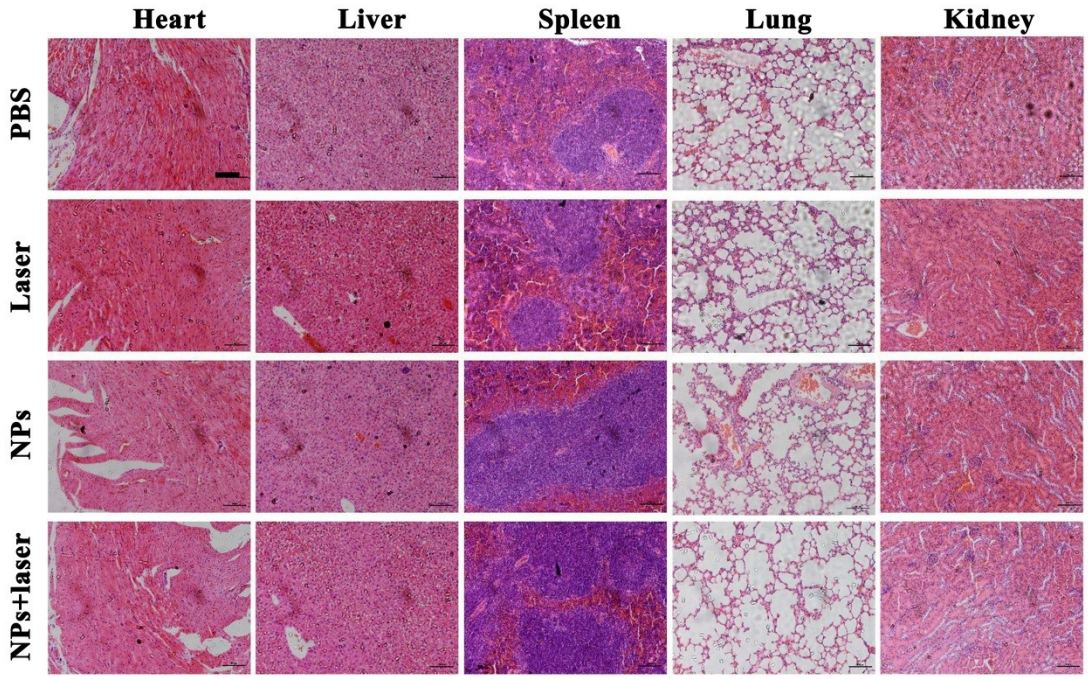

Fig. S12 H&E-strained images of major organs (heart, liver, spleen, lung, and kidney) from 4T1 tumor-bearing mice in different treatment groups. Scale bar: 100 μm.

Reference

1. H. Xie, Z. Li, Z. Sun, J. Shao, X.-F. Yu, Z. Guo, J. Wang, Q. Xiao, H. Wang, Q.-Q. Wang, H. Zhang and P. K. Chu, *Small*, 2016, **12**, 4158-4158.

2. Z. Tang, H. Zhang, Y. Liu, D. Ni, H. Zhang, J. Zhang, Z. Yao, M. He, J. Shi and W. Bu, Adv. Mater., 2017, **29**, 1701683.